

ABSOLUTE MEASUREMENTS OF STARSPOT AREA AND TEMPERATURE:  
II PEGASI IN 1989 OCTOBER

JAMES E. NEFF AND DOUGLAS O'NEAL

Department of Astronomy & Astrophysics, The Pennsylvania State University, 525 Davey Lab, University Park, PA 16802;  
jneff@astro.psu.edu

AND

STEVEN H. SAAR

Harvard-Smithsonian Center for Astrophysics, 60 Garden Street, Cambridge, MA 02138

Received 1995 January 23; accepted 1995 April 25

## ABSTRACT

We are developing an empirical spectrum synthesis technique that yields independent measurements of star-spot filling factor,  $f_S$ , and star-spot temperature,  $T_S$ , by fitting TiO bands of differing temperature sensitivity. The absolute depth of the TiO bands constrains  $f_S$ , while the ratio of their depths is a function only of  $T_S$ . One strength of this technique is its ability to determine the spot parameters in traditionally difficult cases: slowly rotating stars, uniformly spotted stars, and stars that always have spots. For this initial study, we have used a simpler procedure of measuring the band depths in the most spotted star in our survey (the single-lined RS CVn binary system II Pegasi) and for a full grid of comparison stars (inactive G, K, and M dwarfs and giants). This yields  $T_S$  and  $f_S$  for a given assumed temperature of the nonspotted photosphere,  $T_Q$ . The latter was further constrained by the use of simultaneous photometry. We have analyzed a series of spectra of II Peg obtained throughout a single 6.7 day rotational cycle in 1989 October. We find that starspots on II Peg are better modeled by comparison spectra of giants than by dwarfs. Combining TiO analysis with contemporaneous photometry, we find that cool starspots ( $T_S \approx 3500$  K) are always visible, with a fractional projected coverage of the visible hemisphere varying from 54% to 64% as the star rotates. The nonspotted photosphere has a temperature  $T_Q \approx 4800$  K. Our results imply that even at the historical light maximum of  $V = 7.2$ , at least 34% of II Peg was covered by starspots.

*Subject headings:* stars: activity — stars: individual (II Pegasi) — stars: late-type — techniques: spectroscopic

## 1. INTRODUCTION

Photometric and spectroscopic variability of late-type stars has frequently been interpreted as evidence for magnetic activity. The standard picture of stellar activity, inherited from solar observations, includes cool, dark “spots” with enhanced magnetic fields in the photosphere. The immediate cause of these phenomena is a locally closed magnetic-field topology, which suppresses convective energy transport in the photosphere.

Because stellar surfaces are unresolved, these localized phenomena are not directly observable. Most detectable effects are produced by changes in the spot diagnostics integrated over the visible stellar surface, and thus they represent only the asymmetric part of the starspot distribution. The symmetric part of any distribution would escape detection by many current techniques of light-curve and line profile modeling. Therefore, the starspot properties given in the literature often describe only a difference between contrasting regions or entire hemispheres, and not an absolute measure.

In order to devise an absolute measure, we searched for spectroscopic features that would be produced only in starspots. In the spectral region of the molecular bands of TiO, the expected spectrum of starspots is significantly different from that expected of the nonspotted photosphere. The presence of these features in the globally averaged spectrum of stars with a photospheric temperature well above the dissociation temperature of TiO would be incontrovertible evidence for a cool (i.e., starspot) component of the photosphere.

The idea that the TiO bands could be used to measure starspot properties was first stated by Ramsey & Nations (1980)

and by Vogt (1979, 1981a). Ramsey & Nations observed TiO absorption at 8860 Å near the photometric minimum of the G5 IV + K1 IV system V711 Tau (HR 1099). The 8860 Å transition is not produced in dwarfs warmer than  $T \gtrsim 3500$  K (i.e.,  $\sim M2$ ; Wing 1967), so it could not arise in the “normal” photosphere of either star. They concluded that the TiO feature must be produced in spot regions that are at least 1000 K cooler than the unspotted photosphere of the K1 star. Vogt (1981a) showed a ratio of low-dispersion (resolution  $\sim 42$  Å) spectra of II Pegasi (HD 224085) obtained at maximum and minimum light. This ratio spectrum showed strong molecular bands of TiO and VO. Comparing his ratio spectrum with standards, Vogt concluded that the spot’s “equivalent spectral type” was M6 or later. Campbell & Cayrel (1984) marginally detected TiO and CaH molecular absorption in spectra from the Hyades G dwarf star HD 1835. They suggested that a 3% coverage of solar-like spots could explain their observation.

Huenemoerder & Ramsey (1987) attempted a more quantitative study of the effect of spots on the TiO band heads. They found a nonunique solution with a spot coverage of 35%–40% and “equivalent spectral type” M5 for II Peg in 1985, with no phase variation. Huenemoerder (1988) used the same method to derive a spot coverage of 20% for II Peg in 1987 and 10% for UX Ari and V711 Tau. In all cases, the spot “equivalent spectral type” was M6. Huenemoerder, Ramsey, & Buzasi (1989) saw phase-dependent variation in the strength of the 8860 Å TiO band of II Peg in 1988 September. This variation was as expected if the photometric modulation is caused by spots: TiO was strongest at photometric minimum. Combin-

ing their spectra with contemporaneous photometry, they concluded that spots were visible at all phases.

Ramsey & Nations (1980) and Huenemoerder et al. (1989) observed only one TiO band (8860 Å), so it was impossible to separate the effect of increasing spot coverage from decreasing  $T_s$ . Furthermore, the nonspot photosphere was represented by a "standard" G or K star spectrum of the same spectral type as the spotted star, and the selection of spot comparison spectra was limited. On the positive side, these intriguing results helped prove the hypothesis that starspots cause most of the photometric variability long observed from RS CVn and BY Dra systems. They conclusively demonstrated that cool and warm photospheric regions must coexist on the same stars, as seen to a much smaller degree on the Sun. Measurement of enhanced magnetic flux in "starspots" will be the proof that these cool regions are indeed sunspot analogs. Such evidence is beginning to emerge (Saar, Piskunov, & Tuominen 1992, 1994; Donati et al. 1990, 1992).

Inspired by these pioneering studies, we began a program to use the TiO bands to systematically measure starspot areas ( $f_s$ ) and temperatures ( $T_s$ ) on late-type stars (preliminary results were given by Saar & Neff 1990; Neff, O'Neal, & Saar 1992; O'Neal, Neff, & Saar 1994). For our targets, we selected a group of stars that were previously expected to be spotted (dwarf BY Dra variables and subgiant/giant RS CVn binaries). We also selected a sample of inactive G and K stars spanning the spectral type range of our target stars to represent the inactive photosphere and a sample of M stars to approximate the starspot photosphere. To investigate the effect of surface gravity, we included both giant and dwarf comparison stars.

We use spectra of the 7055 Å and 8860 Å TiO bands to measure independently the area and the temperature of starspots. As a result of different temperature sensitivities (e.g., Pettersen & Hawley 1989), the relative absorption strength of the bands constrains  $T_s$ , while their absolute strength is a function of  $f_s$ .

We report here the first results obtained using a full grid of comparison star spectra. We have chosen the highly spotted star II Pegasi for this initial study. We measure  $f_s$  on II Peg as a function of rotational phase, and we derive a mean  $T_s$ . In future papers in this series, we will develop the more sophisticated spectrum synthesis techniques required for less heavily spotted stars, investigate in detail the limitations and capabilities of these techniques, give results for heavily spotted stars over rotational and cycle timescales, and compile a catalog of starspot areas and temperatures for a wide range of late-type stars.

## 2. OBSERVATIONS AND DATA REDUCTION

### 2.1. Selection of a Comparison Grid

Our method requires that we obtain high-quality spectra of several categories of "inactive" stars (Table 1). Spectra of inactive G and K dwarfs represent unspotted photosphere (hereinafter referred to as "quiet"). Spectra of M giants and M dwarfs represent spectra of starspots (hereinafter referred to as "spot"). Our quiet grid covers  $T_{\text{eff}} = 4325\text{--}5600$  K, and our spot grid covers  $T_{\text{eff}} = 3000\text{--}3850$  K (dwarfs) and  $T_{\text{eff}} = 3050\text{--}3650$  K (giants). Steps in  $T_{\text{eff}}$  were typically less than 200 K for the quiet grid and  $\leq 75$  K for the spot grid. Effective temperatures were estimated from the average of a  $T_{\text{eff}}$  versus  $(B-V)$  color relation (Gray 1988) and a  $T_{\text{eff}}$  versus  $(R-I)_J$  color relation (Johnson 1966) for the quiet comparison stars. The  $T_{\text{eff}}$  versus  $(R-I)_{\text{KC}}$  relation of Bessell (1991) was used for

the spot comparison dwarfs, while the  $T_{\text{eff}}$  versus  $(V-K)$  calibration of Ridgway et al. (1980) was used to determine  $T_{\text{eff}}$  for the giants. Photometry for the objects came from Stauffer & Hartmann (1986), the Bright Star Catalog (Hoffleit & Jaschek 1982), and the Gliese (1969) catalog.

### 2.2. The Observations

The data were obtained during 10 observing runs at the National Solar Observatory's McMath-Pierce telescope. They consist of 617 medium-resolution ( $\lambda/\Delta\lambda \approx 14,000$ ), high-S/N (200–400) spectra with a range of approximately 200 Å centered on the TiO bands beginning at 7055 Å [the 7055, 7088, and 7126 Å bands of the  $\gamma(0,0)$  system] and on the band at 8860 Å [the strongest of the  $\delta(0,0)$  system]. We observed 10 dwarf and 16 subgiant/giant target stars, 11 inactive G and K stars, and 13 giant and 18 M dwarf comparison stars. All the comparison stars were observed on at least two separate nights.

The 1.5 m McMath-Pierce telescope was designed for solar observations, but it has been adapted for nighttime spectroscopic use (Smith & Jaksha 1984). The success of our project is due in large part to the flexible scheduling provided by the "solar-stellar" program (permitting us, for example, to observe over 2 yr span the large number of comparison stars necessary before the analysis could begin). The primary components of the stellar spectrograph system (Smith & Giampapa 1987), as configured for our program, are (1) a five-slice Bowen-Wahlravn image slicer, (2) a Milton & Roy reflection grating with 1200 grooves  $\text{mm}^{-1}$  used in first order, (3) a filter (Schott OG570) to remove contributions from higher orders, (4) a 105 mm Nikon transfer lens, and (5) a Texas Instruments 800 × 800 CCD (15  $\mu\text{m}$  square pixels). We used a quartz lamp incident on the image slicer for flat-fielding and various Th-Ar and Th-Ne lamps for wavelength calibration.

### 2.3. II Pegasi

In this paper, we discuss only one of our targets, II Pegasi (HD 224085), selected as the most illustrative example of a highly spotted star. II Peg is a single-lined, spectroscopic binary system with a spectral type K2–3 IV–V and a  $v \sin i$  of 21  $\text{km s}^{-1}$ . The secondary star has never been observed, but it probably is a low-mass dwarf [mass function  $f(m) = 0.035$ ]. Unless otherwise noted, we use the system parameters from the Strassmeier et al. (1993) catalog. For comparison with contemporaneous photometry and with previous papers, we use the ephemeris determined by Vogt (1981a) and confirmed more recently by Byrne et al. (1989):  $\Phi_{\text{orb}} = \text{JD } 2,443,033.47 + 6.72422E$ . With this ephemeris,  $\Phi = 0$  occurs at superior conjunction (i.e., primary star farthest away from observer).

II Peg is one of the most spotted stars known. Its light curve has been analyzed over several decades (Hartmann, Londoño, & Phillips 1979; Cutispoto & Rodonò 1992) and can change radically from one year to the next (e.g., Byrne 1992; Doyle et al. 1988). It can exhibit  $V$ -band variations ranging from 0 to 0.6 mag, and its light curve can be sinusoidal or irregular. Color variations up to 0.06 in  $(V-R)$  have been seen, with the darkest phases also being the reddest, consistent with the starspot hypothesis (Doyle et al. 1992a). The brightest observed  $V$ -band magnitude of 7.2 (Rucinski 1977) is often assumed to indicate the "immaculate" (i.e., unspotted) level of II Peg. All previous determinations of starspot area have modeled light curves (e.g., Rodonò et al. 1986; Eaton 1992) using large monolithic spots and have assumed an immaculate level. The results,

TABLE 1  
PROPERTIES OF COMPARISON STARS AND MEASURED BAND DEPTHS

HD	HR	Other Names	Spectral Type	$V$	$(R-I)$	$(B-V)$	$T_{\text{eff}}$	$D_{7055}^a$	$D_{8860}^a$
"Quiet" Comparison Stars									
20630	996	$\kappa$ Cet	G5 V	4.8	0.22	0.68	5600	...	...
101501	4496	61 UMa	G8 V	5.3	0.27	0.72	5550	...	...
149661	6171	12 Oph	K2 V	5.8	0.26	0.82	5300	...	...
185144	7462	$\sigma$ Dra	K0 V	4.7	0.29	0.79	5300	...	...
26965	1325	40 Eri A	K1 V	4.4	0.31	0.82	5175	...	...
22049	1084	$\epsilon$ Eri	K2 V	3.7	0.30	0.88	5050	...	...
160346		Gl 688	K3 V	6.5	0.34	0.96	4850	...	...
16160	753		K3 V	5.8	0.36	0.98	4775	...	...
32147	1614		K3 V	6.2	0.35	1.06	4750	...	...
131977	5568		K4 V	5.7	0.42	1.11	4575	...	...
201091	8085	61 Cyg A	K5 V	5.2	0.47	1.18	4325	...	...
Giant "Spot" Comparison Stars									
42995	2216	$\eta$ Gem	M3 III	3.3	1.31	1.60	3650	37.7	8.5
44478	2286	$\mu$ Gem	M3 III	2.9	1.38	1.64	3625	39.5	10.3
20720	1003		M3.5 III	3.7	1.46	1.62	3600	41.5	8.9
2411	103	TV Psc	M3 III	5.1	1.54	1.65	3575	53.6	17.1
175588	7139	$\delta$ -2 Lyr	M4 II	4.3	1.63	1.68	3550	50.3	20.3
123657	5299	BY Boo	M4.5 III	5.3	1.66	1.59	3550	45.9	17.2
113866	4949	FS Com	M5 III	5.6	1.81	1.59	3475	61.1	35.6
175865	7157	R Lyr	M5 III	4.0	1.91	1.59	3425	51.2	21.6
172380	7009	XY Lyr	M5 II	6.0	1.96	1.65	3400	56.6	25.6
94705	4267	VY Leo	M5.5 III	5.8	2.09	1.45	3325	52.5	22.5
18191	867	RZ Eri	M6 III	5.9	2.17	1.47	3200	62.1	38.0
41698	2156	S Lep	M6 III	7.0	2.37	1.63	3125	65.1	41.4
117287	5080	R Hya	M7 III	5.0	2.42	1.60	3050	66.4	52.3
Dwarf "Spot" Comparison Stars									
201092	8086	Gl 820B	K7 V	6.0	0.60	1.37	3850	4.3	0.5
88230		Gl 380	K7 V	6.6	0.60	1.36	3825	8.1	1.3
28343		Gl 169	K7 V	8.3	0.62	1.35	3750	11.3	0.9
		Gl 186	K5 V	9.3	0.64	1.28	3725	8.9	2.1
11631		Gl 488	M0.5 V	8.5	0.66	1.40	3700	11.9	2.1
79210		Gl 388A	M0 V	7.6	0.68	1.39	3675	10.0	0.2
79211		Gl 388B	M0 V	7.7	0.69	1.42	3650	11.0	1.2
32450		Gl 185	M0 V	8.5	0.72	1.41	3625	12.3	1.3
		Gl 400	M2 V	9.3	0.74	1.41	3600	12.6	2.2
		Gl 96	M1.5 V	9.4	0.78	1.49	3525	16.3	3.9
42581		Gl 229	M1 V	8.1	0.82	1.50	3450	19.4	3.1
36395		Gl 205	M1.5 V	8.0	0.85	1.47	3400	22.5	5.3
1326		Gl 15	M2 V	8.1	0.88	1.56	3375	19.2	2.8
95735		Gl 411	M2 V	7.5	0.91	1.51	3350	22.2	6.5
		Gl 393	M2.5 V	9.6	0.95	1.52	3325	28.4	5.9
		Gl 251	M4 V	10.0	1.09	1.57	3250	33.2	9.3
		Gl 273	M4 V	9.9	1.19	1.56	3175	42.6	14.1
		Gl 699	M5 V	9.6	1.25	1.74	3000	38.2	7.6

<sup>a</sup> Band depth index, in percent of continuum level; defined in § 3.2.

ranging from  $f_S = 0\%$  to  $60\%$ , are thus only lower limits to the true spot coverage.

II Peg is a prototype for the current paradigm of stellar activity. Ultraviolet line fluxes obtained in 1981 showed a dramatic anticorrelation with the visible magnitude (Rodonò et al. 1987). Follow-up studies in 1983 and 1986, however, failed to show such correlations (Andrews et al. 1988; Doyle et al. 1989). II Peg is a radio source (Drake, Simon, & Linsky 1989) and an X-ray source (Dempsey et al. 1993). In 1989 August, a large flare was detected simultaneously in X-rays, spectral lines, and, unusual for an RS CVn system (see Saar, Nordström, & Andersen 1990), in visible-band photometry (Doyle et al. 1992a; Doyle, van den Oord, & Kellett 1992b). II Peg has previously been observed to flare in visible spectra (e.g., Huenemoerder, Buzasi, & Ramsey 1990), ultraviolet spectra (Neff 1991),

extreme ultraviolet (Patterer et al. 1993), and X-rays (Schwartz et al. 1981; Tagliaferri et al. 1991).

We observed II Peg throughout a single rotational/orbital cycle in 1989 October (see Table 2). With one exception, we observed in both wavelength bands on each of six consecutive nights. On the night of 1989 October 11 there was H I and He I line emission above the local continuum, suggesting the occurrence of a large flare.

#### 2.4. Reduction of the McMath-Pierce Spectra

As an image slicer forms the entrance aperture to the McMath-Pierce stellar spectrograph, the data are somewhat "nonstandard," and we describe our procedures in detail. Five parallel slices, each with an effective width of approximately  $1''$ , are spread over about 40 rows of the CCD, with the spectra



TABLE 2  
LOG OF McMATH-PIERCE OBSERVATIONS OF II PEG

Date	Band	UT Start	Exposure (s)	JD (midexposure)	$\Phi^a$ (midexposure)	Notes
1989 Oct 9 .....	7055	0448	1800	2,447,808.711	0.16	
	8860	0744	3600	2,447,808.844	0.18	
1989 Oct 10 .....	7055	0344	2100	2,447,809.668	0.30	
	8860	0820	3600	2,447,809.867	0.33	
1989 Oct 11 .....	8860	0609	3600	2,447,810.777	0.46	Flare
	7055	0757	2100	2,447,810.844	0.47	Flare
1989 Oct 12 .....	7055	0817	2700	2,447,811.859	0.62	
1989 Oct 13 .....	7055	0602	2100	2,447,812.762	0.76	
	8860	0824	2700	2,447,812.867	0.77	
1989 Oct 14 .....	7055	0630	1500	2,447,813.781	0.91	
	8860	0853	3000	2,447,813.887	0.93	

<sup>a</sup> Orbital phase computed from HJD 2,443,033.47 + 6.72422E.

aligned along columns. We used four-row on-chip summing, but even with no summing, there is overlap between the slices. The resultant  $25 \times 800$  images were written to FITS files at the telescope, and all further reduction was done using IDL programs at Penn State University. The image slicer complicates flat-fielding and extraction, because the flat-field lamp is always uniformly incident over the entire face of the slicer, while starlight can fall over an area that varies with telescope pointing, seeing, guiding precision, and even color and air mass (because of the dichroic filter in the automatic guider system). After bias subtraction and careful flat-fielding, an “optimal” extraction was performed.

Because of the TiO band heads and the aforementioned flat-fielding problems, continuum normalization of the M star and target star spectra is not straightforward. We applied a spline fit to the continuum blueward of the 7055 Å and 8860 Å band heads. We then linearly extrapolated the spline fit redward from the band head. As a result of the bands, normalization at the longest wavelengths in both regions is less accurate. Because the measurements in this paper are performed only at the band head, this will not affect our results.

Three different wavelength calibration lamps were used during the 2 years that our observations were obtained. One of these was a Th-Ne lamp that provided very few lines in our region of interest. Fortunately, the polynomial fits to the Th-Ar comparison spectra indicated that the dispersion is quite linear over the 200 Å range of the TI CCD. Therefore we used a linear wavelength solution using comparison lamp spectra obtained within a few hours of each stellar spectrum. All spectra were then interpolated onto a common wavelength scale. The mean dispersion was  $0.281 \text{ Å pixel}^{-1}$  at 7055 Å and  $0.260 \text{ Å pixel}^{-1}$  at 8860 Å. The mean resolution determined from the comparison lamp line widths was 1.7 pixels FWHM at 7055 Å and 2.5 pixels at 8860 Å, varying between runs by  $\pm 0.4$  pixels depending on spectrograph focus.

To remove the effects of varying amounts of water vapor and different air masses on the spectra, we developed an interactive “drying” program. We used a very high S/N spectrum of a hot star to provide a (nearly) featureless continuum (a high-order polynomial was fitted to the 8860 Å bandpass to remove Paschen- $\theta$  and Paschen- $\iota$  lines of H  $\gamma$ ). These “telluric line” spectra, when normalized, were interactively overplotted on our reduced spectra in an animation mode—simultaneously showing the “wet” spectrum, the telluric lines growing or shrinking (depending on keyboard input), and the resultant “dry” spectrum. In a procedure similar to focusing, the user

rapidly decides upon the correct telluric line scaling factor, and telluric effects are removed.

The reduced spectra for our comparison stars are shown in Figures 1–3. The 1989 October II Peg spectra are shown in Figure 4.

### 3. ANALYSIS

#### 3.1. Spectrum Synthesis Model

The two wavelength regions we selected contain TiO absorption bands with different temperature sensitivities: the 7055 Å bands first become visible for an immaculate dwarf star at spectral type about K5, while the 8860 Å band is not evident until M2V (Wing 1967). Modeling the two bands simultaneously permits an estimate of both the area (from the absolute band strengths) and the temperature (from the band strength ratio) of cool spots on the stellar surface. Our approach (based on that of Huenemoerder & Ramsey 1987) is to model the normalized spectrum from a spotted star ( $F_{\text{total}}$ ) as the weighted sum of  $F_S$  and  $F_Q$ , the spectra of suitable standard stars with  $T_{\text{eff}} = T_S$  and  $T_{\text{eff}} = T_Q$ , respectively. The model is given by

$$F_{\text{total}} = \frac{f_S R_\lambda F_S + (1 - f_S) F_Q}{f_S R_\lambda + (1 - f_S)}, \quad (1)$$

where  $f_S$  is the total fractional projected area of spots on the observed hemisphere weighted by limb darkening (essentially the flux-weighted filling factor), and  $R_\lambda$  is the continuum surface flux ratio between the spot and the quiet photosphere. To compute  $R_\lambda$ , we used models of Kurucz (1991) for  $\log g = 4$ , the approximate surface gravity of II Peg. We averaged the continuum fluxes from models with  $T_{\text{eff}}$  between 3500 and 6500 K over 20 Å bandpasses just blueward of the positions of the 7055 Å and 8860 Å band heads. The relationship between  $\log(T_{\text{eff}})$  and  $\log(\langle F \rangle)$ , the average continuum flux in the given bandpass at a given  $T_{\text{eff}}$ , was approximated by a quadratic relationship to the Kurucz values. To compute  $R_\lambda$  for  $T_S$  as low as 3000 K, we extrapolated this relationship to lower  $T_{\text{eff}}$ .

#### 3.2. Empirical Band Depth Index

We define a band depth index,  $D_\lambda$ , for each spectrum as the difference between pseudocontinuum levels on either side of the band head, expressed as a percent of the continuum level. To remove the effects of atomic lines in the definition, we averaged the five highest intensity values within 5 Å bandpasses

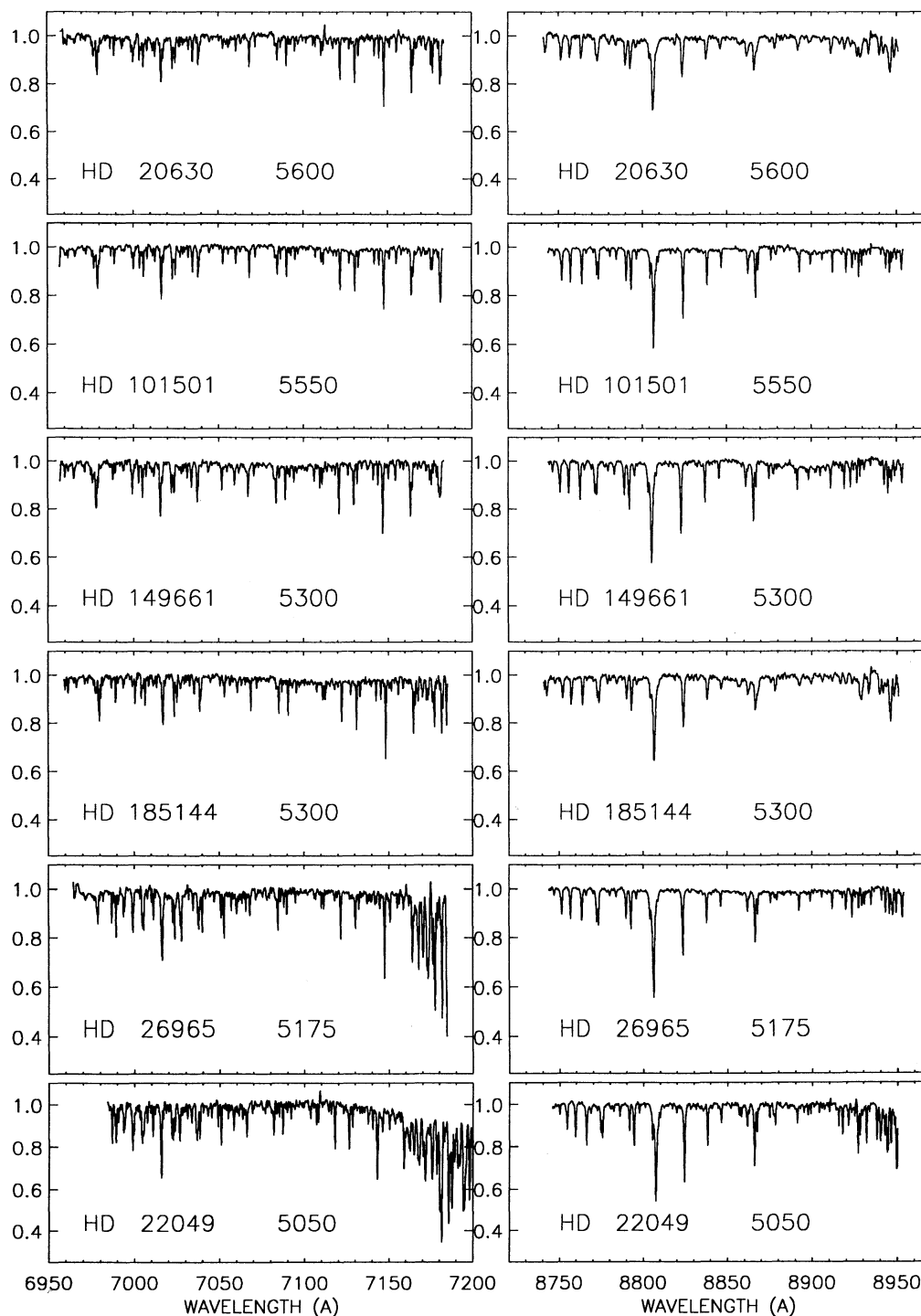


FIG. 1.—Sample quiet comparison spectra near the 7055 Å (left) and 8860 Å (right) TiO bands, in order of decreasing  $T_{\text{eff}}$  (which is given along with the star identification in each panel). All spectra are plotted on the same continuum-normalized scale. All comparison stars were observed at least twice.

centered within  $\pm 5$ – $10$  Å of the band head. The regions we used to determine  $D_{7055}$  were 7043–7048 Å and 7060–7065 Å, while for  $D_{8860}$  we used 8850–8855 Å and 8871–8876 Å. We measured this index for both bands for II Peg (Table 3) and for all spectra of the comparison stars (see Table 1). Since all comparisons were observed more than once, the average of the band depth measurements for each comparison star was used. The  $D_{\lambda}$  values of the comparison stars are plotted in Figure 5,

showing an approximately linear increase with decreasing  $T_{\text{eff}}$  over this temperature range.

Our definition of band depth differs from that of Huene-moerder et al. (1989), who measured the difference between the pseudocontinuum level and the level in the middle of the absorption band. In practice, it is difficult to determine the location of the middle of the band in our single-order spectra. Our band depths would be systematically greater than those of

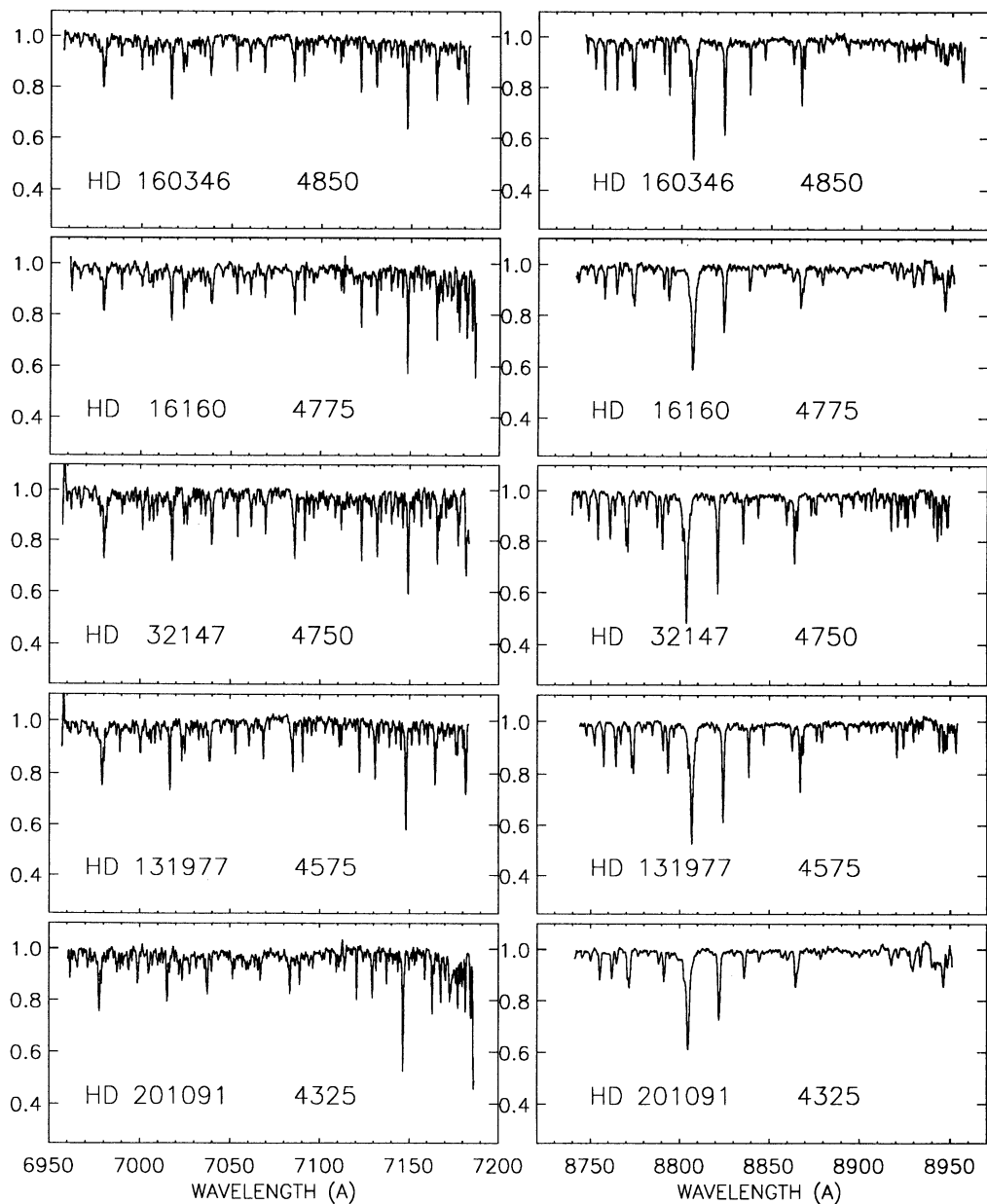


FIG. 1—Continued

TABLE 3  
BAND DEPTH INDICES AND DERIVED  $f_s$  VALUES FOR II PEG

DATE	$\Phi_{\text{orb}}$	$D_{7055}$	$D_{8860}$	$D_{7055}/D_{8860}$	$f_s^a$			
					$T_Q = 4500;$ $T_S = 3500$	$T_Q = 4800;$ $T_S = 3500$	$T_Q = 5100;$ $T_S = 3500$	$T_Q = 4850;$ $T_S = 3500^b$
Oct 9 .....	0.17	4.8	3.1	1.5	46	54	61	72
Oct 10 .....	0.32	5.0	3.9	1.3	50	58	65	68
Oct 11 .....	0.47	... <sup>c</sup>	... <sup>c</sup>	... <sup>c</sup>	... <sup>c</sup>	... <sup>c</sup>	... <sup>c</sup>	... <sup>c</sup>
Oct 12 .....	0.62	6.2	... <sup>d</sup>	... <sup>d</sup>	54	62	69	71
Oct 13 .....	0.77	6.3	4.5	1.4	56	63	70	77
Oct 14 .....	0.92	6.6	4.9	1.3	56	64	72	76

<sup>a</sup> Values in percent of visible hemisphere.

<sup>b</sup> Best-fit synthetic photometry.

<sup>c</sup> Uncertain as a result of flare emission.

<sup>d</sup> No 8860 Å observations on Oct 12.

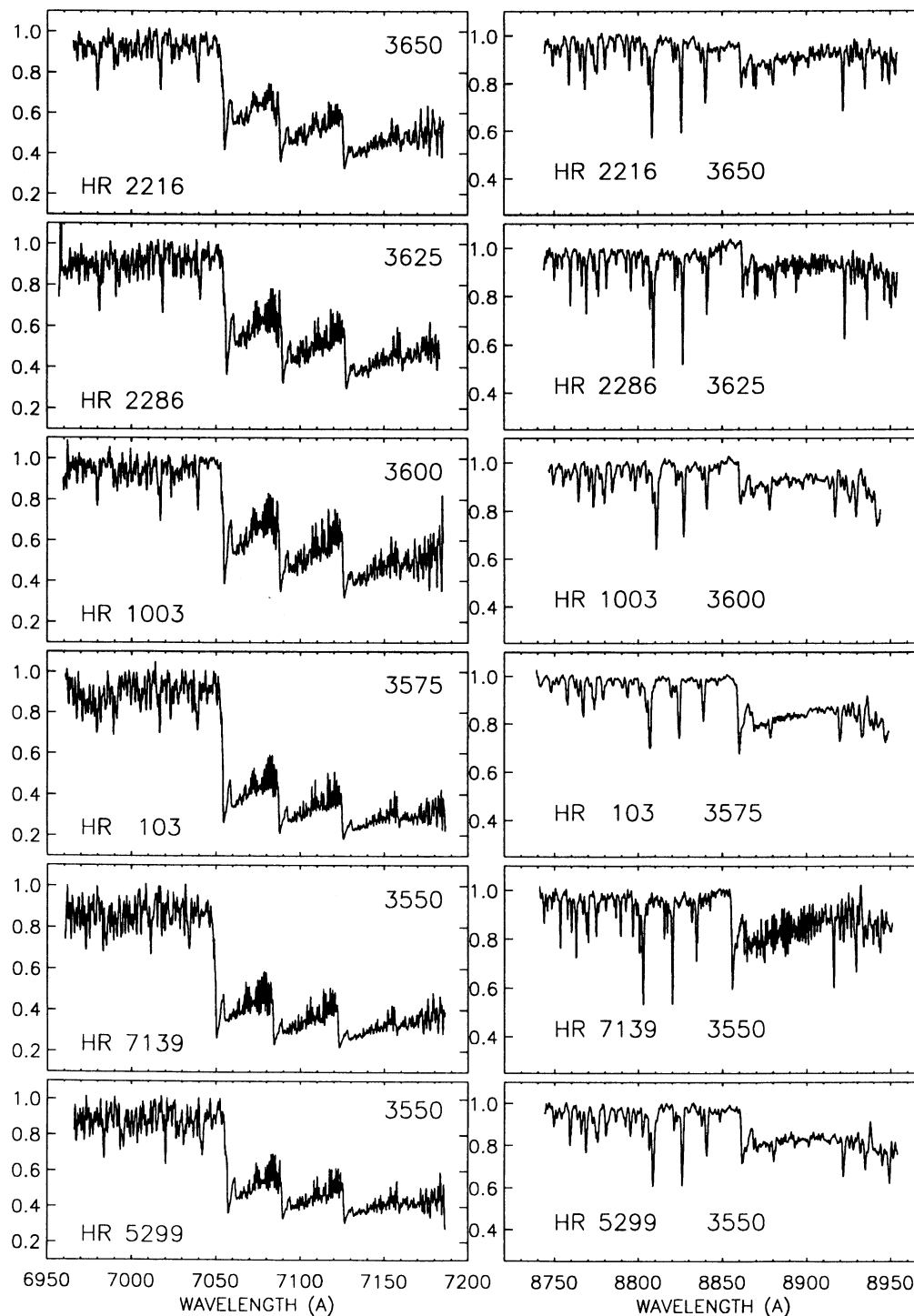


FIG. 2.—Sample spot comparison spectra of M giant stars near the 7055 Å (*left*) and 8860 Å (*right*) TiO bands, in order of decreasing  $T_{\text{eff}}$ . All spectra are plotted on the same continuum-normalized scale. All comparison stars were observed at least twice.

Huenemoerder et al. (1989) as a result of the positive (with wavelength) slope within the absorption band.

With this definition, we can effectively replace  $F_S$  in equation (1) by a step function that has a value of unity to the left of the band head and  $1 - D_\lambda$  to the right of the band head, with  $F_Q$  set to unity. Equation (1) can then be expressed in terms of our  $D_\lambda$  parameter, yielding a predicted depth for any combination of  $T_S$ ,  $T_Q$ , and  $f_S$ .

### 3.3. Variation of Band Depth with Surface Gravity

The ratio of the strengths of the two bands,  $D_{7055}/D_{8860}$ , is primarily a function of  $T_{\text{eff}}$ . On the nights when we could measure it (excluding October 11, the date of the flare), this ratio was between 1.3 and 1.55 for II Peg (see Table 3). Using the measured band depth ratios in our M dwarf comparison spectra, we are unable to reproduce a depth ratio below 3 (see

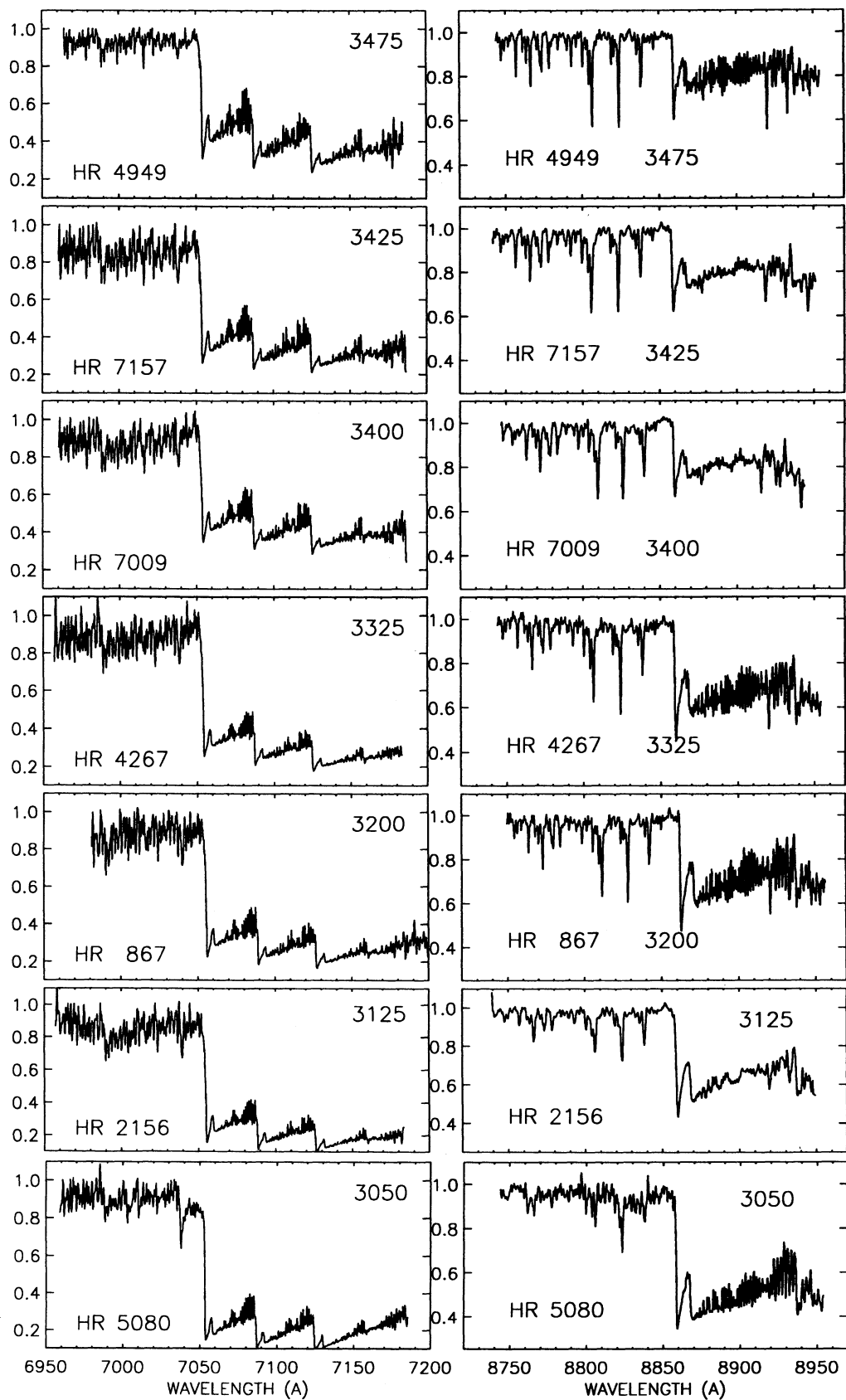


FIG. 2—Continued



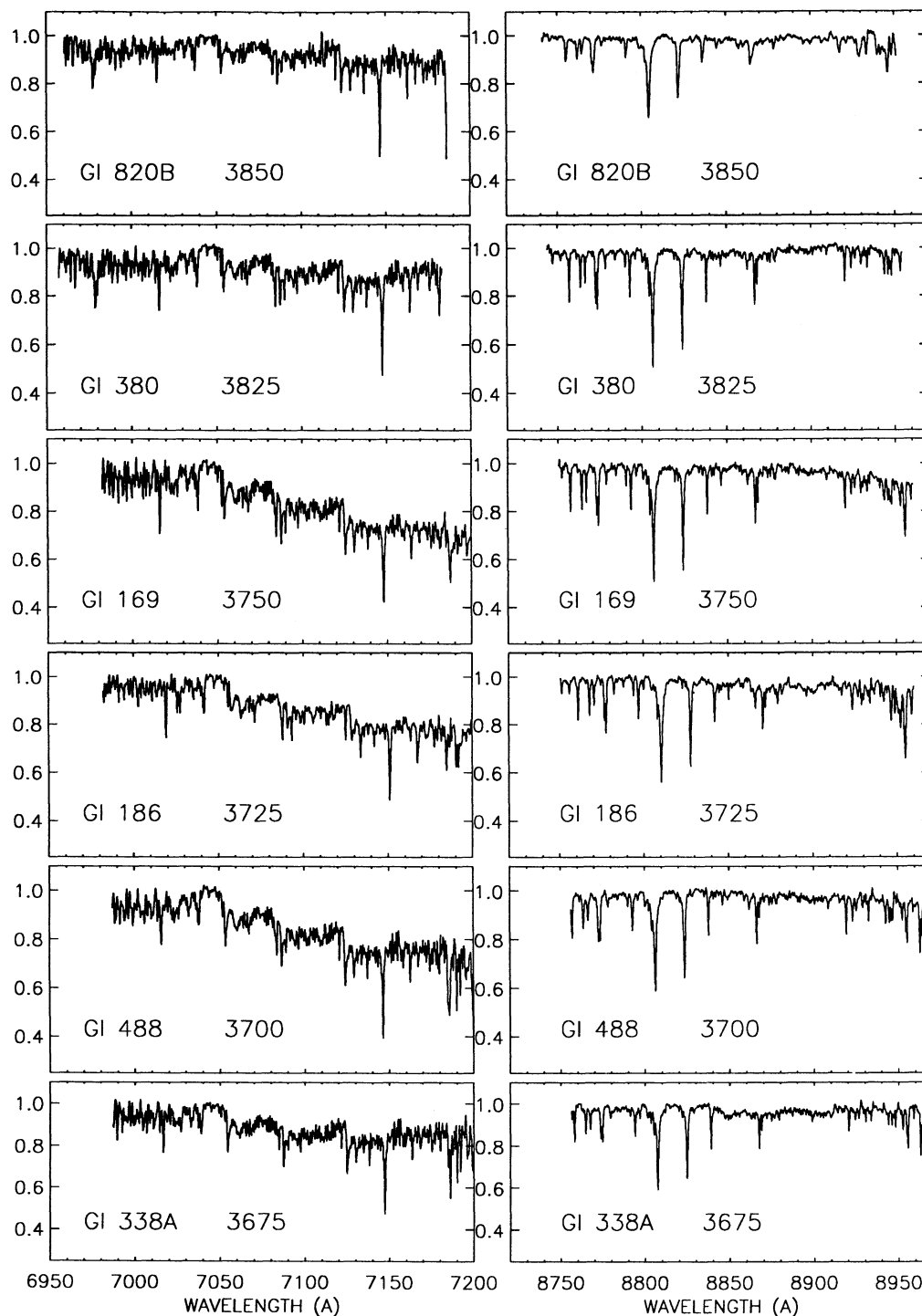


FIG. 3.—Sample spot comparison spectra of M dwarf stars near the 7055 Å (left) and 8860 Å (right) TiO bands, in order of decreasing  $T_{\text{eff}}$ . All spectra are plotted on the same continuum-normalized scale. All comparison stars were observed at least twice.

Table 1). Even models using  $T_s = 2700$  K (linearly extrapolated from the  $D_\lambda$  vs.  $T_{\text{eff}}$  relationship) cannot produce a depth ratio below 2. On a star with  $T_Q \geq 4700$  K, a spot with  $T_s$  this low would be unable to produce the observed TiO band variations, because the spot continuum is too dark ( $R_\lambda \leq 0.027$  at 7055 Å). Therefore, spectra of M dwarfs cannot provide a good model for the starspots on II Peg.

Spot comparison spectra using giant stars, on the other

hand, can reproduce the band ratios observed on II Peg. We find that for a given  $T_{\text{eff}}$ ,  $D_{8860}$  is approximately 5 times larger in a giant than an M dwarf, while  $D_{7055}$  is 1.5–2 times greater in giant stars (Fig. 5). The spectral type of II Peg is generally quoted in the range K2–3 IV–V (see Strassmeier et al. 1993 for references). Thus, neither the giant nor dwarf spot comparison grid can be considered ideal. Nevertheless, we have used the M giant spectra to model II Peg spots in the following analysis.

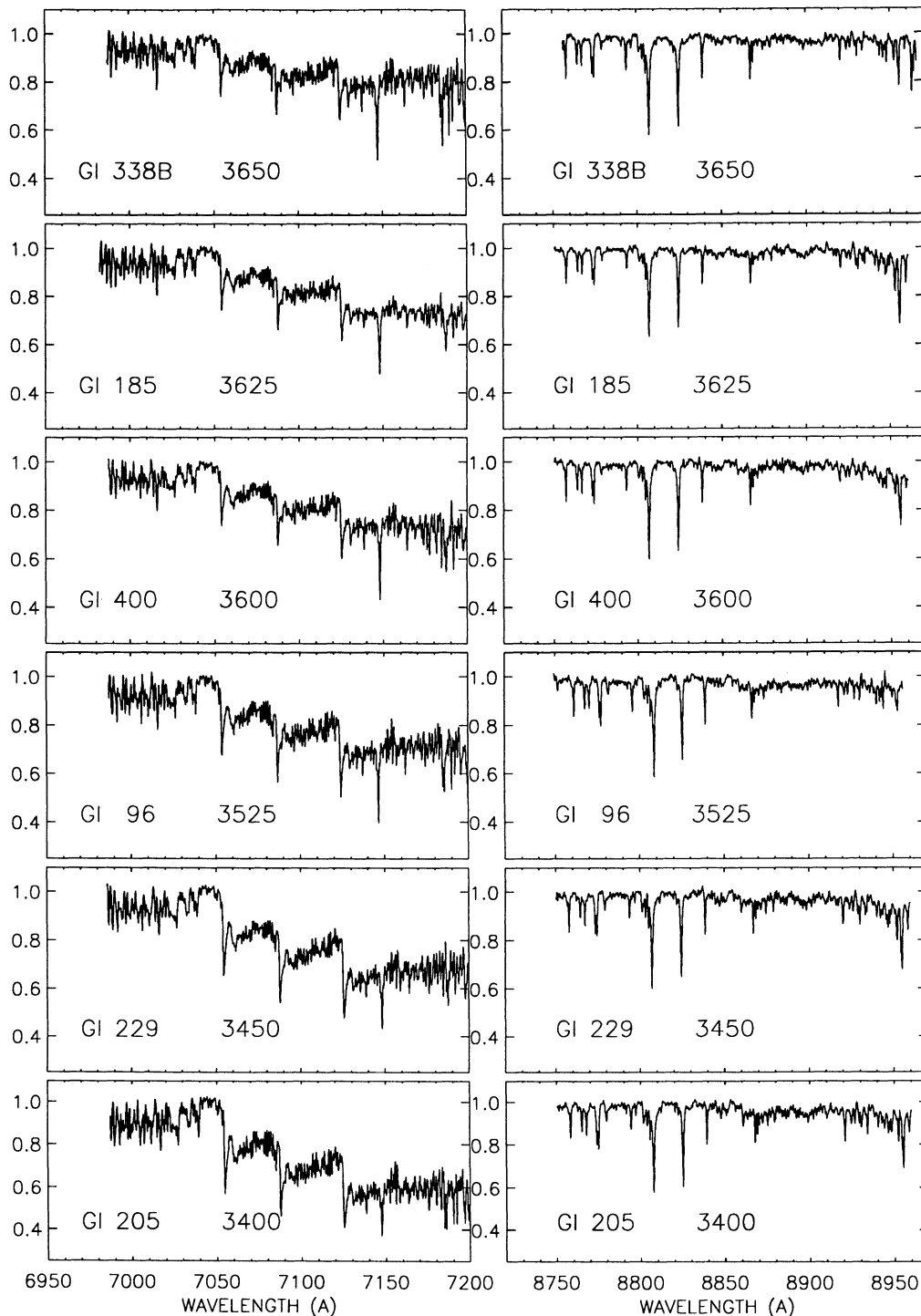


FIG. 3—Continued

### 3.4. Derivation of $T_S$

We used equation (1) and the measured  $D_\lambda$  values of the comparison stars to predict band depths for a uniform three-dimensional grid of input stellar parameters ( $T_Q$ ,  $T_S$ , and  $f_S$ ). In order to remove scatter and transform to a uniform temperature grid, we first used the measured  $D_\lambda$  values to derive the temperature dependence of each band depth. For the leading band in the 7055 Å region, the best linear fit to the

empirical  $D_{7055}$  versus  $T_{\text{eff}}$  relationship (see Fig. 5) for giants is given by

$$D_{7055}^G = -0.4420 \frac{T_{\text{eff}}}{1000} + 2.040, \quad (2)$$

with an rms deviation of 0.051. In the 8860 Å band, the best linear fit is given by

$$D_{8860}^G = -0.6637 \frac{T_{\text{eff}}}{1000} + 2.520, \quad (3)$$

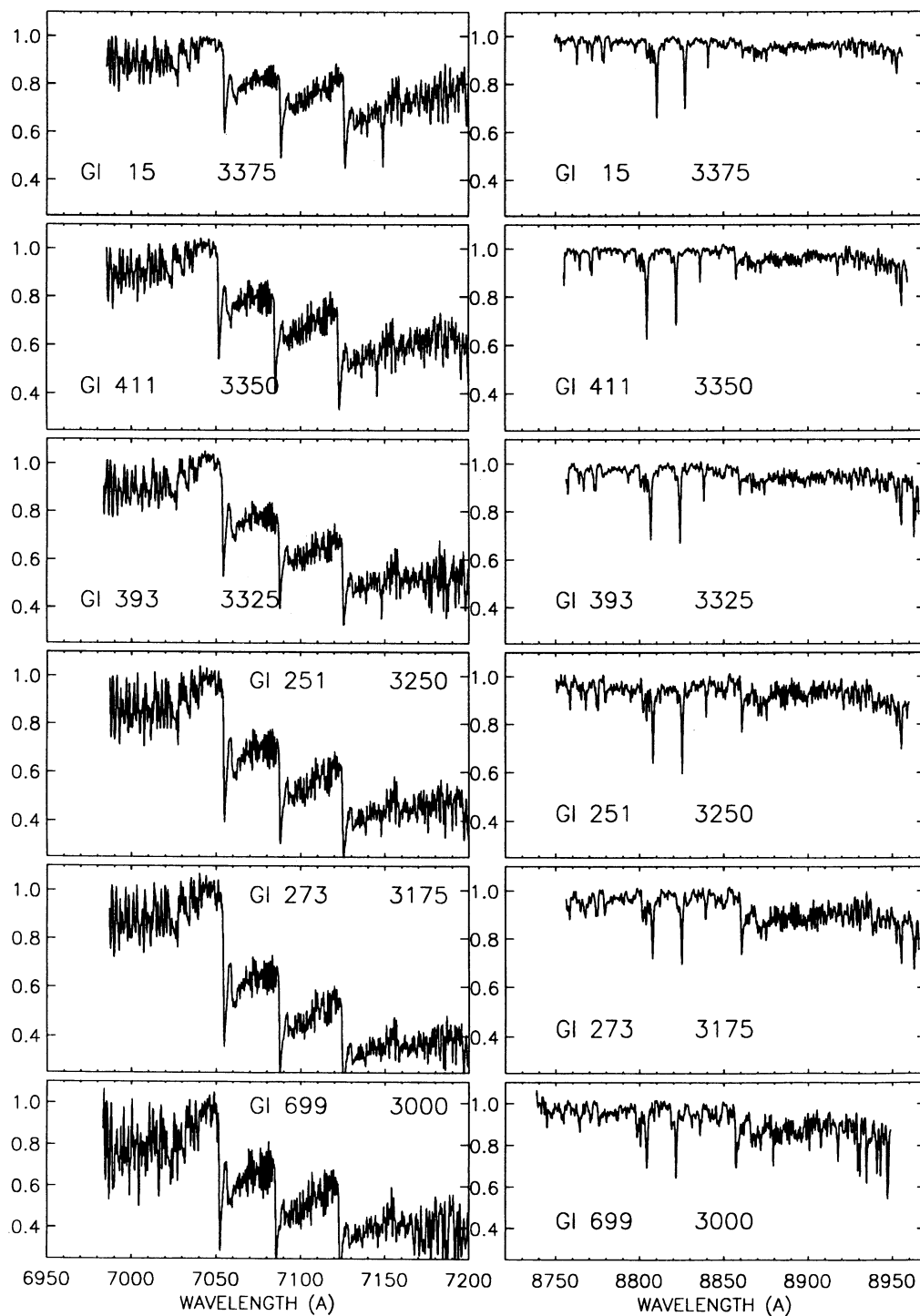


FIG. 3—Continued

with an rms deviation of 0.058. For completeness, we also present the linear fits to the depths of the M dwarf stars:

$$D_{7055}^D = -0.4382 \frac{T_{\text{eff}}}{1000} + 1.722, \quad (4)$$

and

$$D_{8860}^D = -0.1288 \frac{T_{\text{eff}}}{1000} + 0.4921. \quad (5)$$

The linear fits presented here are valid only over the  $T_{\text{eff}}$  range of our data. Ramsey (1981) conducted a thorough study of the behavior of the 8860 Å band over a larger  $T_{\text{eff}}$  range, using K and M giants. At lower temperatures  $D_{\lambda}$  eventually saturates at a constant value, and at higher temperatures the molecule eventually dissociates (or the absorption becomes too weak to reliably measure  $D_{\lambda}$ ). The data can be better fitted with bilinear or higher order representations, but we do not feel that such fits are more realistic than these linear fits.

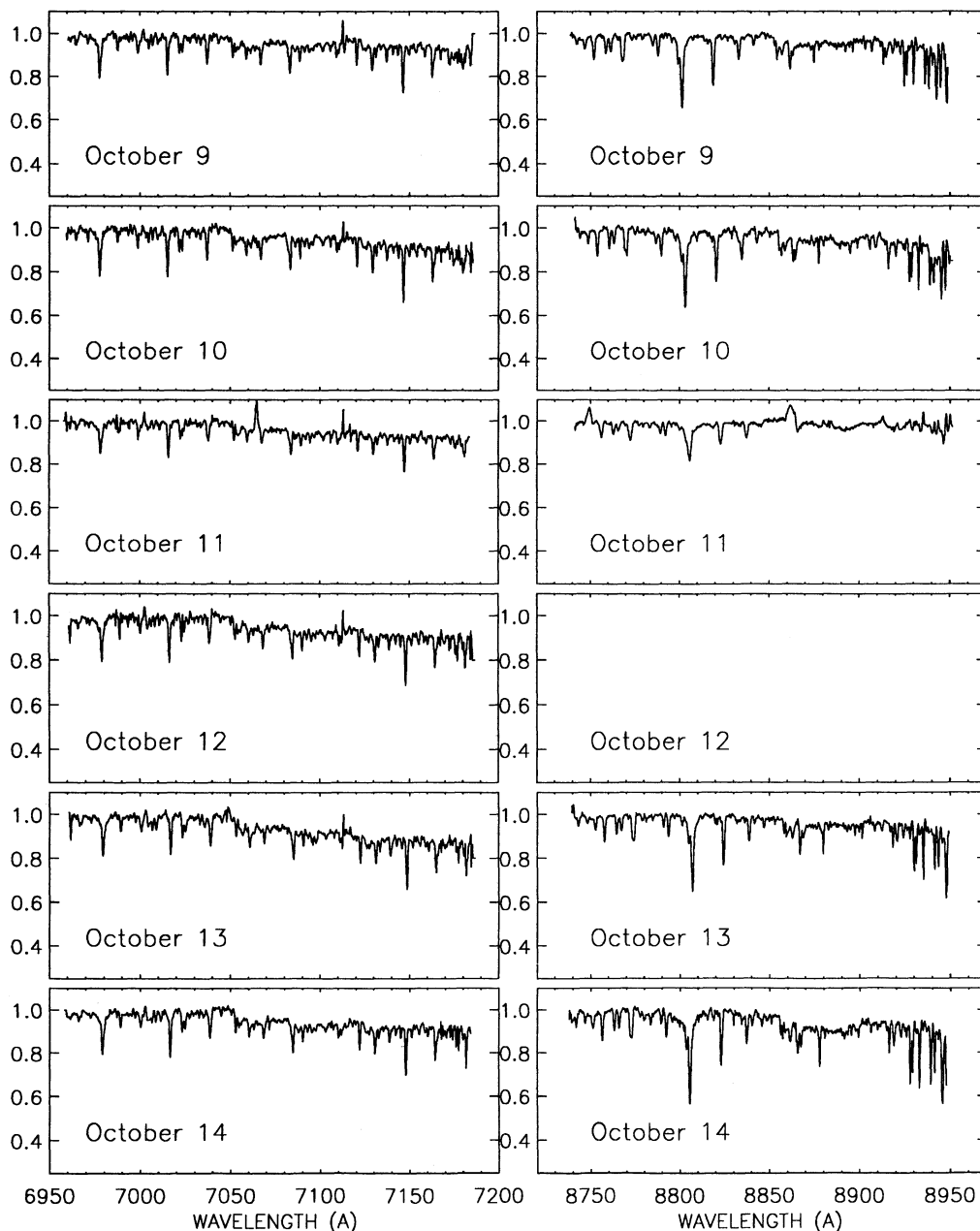


FIG. 4.—Reduced II Peg spectra near the 7055 Å (left) and 8860 Å (right) TiO bands. The spectra are in temporal order from 1989 October 9 to 1989 October 14. Note the flare in three emission lines on 1989 October 11. No 8860 Å data were obtained on 1989 October 12.

We then generated a table of predicted band depths for every combination of  $T_S$  (in steps of 50 K over our entire range),  $f_S$  (in steps of 10%, but with “best-fit” values interpolated between these grid points), and  $T_Q$  (covering the range of interest for all our stars, with steps of 50 K). Using both bands, we find that  $T_S$  was uniquely constrained (because the band depth ratio is a function solely of temperature). However, a large range of  $T_Q$  and  $f_S$  can yield the same absolute band depths.

### 3.5. Estimates of $T_Q$ and $f_S$

We are able to uniquely determine  $T_S$ , assuming only that all spots have the same temperature. We cannot independently determine  $T_Q$  and  $f_S$  from our data, but we can derive a simple

relationship between them. This indeterminacy arises because we are essentially trying to determine three parameters ( $T_S$ ,  $T_Q$ , and  $f_S$ ) from only two independent measurements ( $D_{8860}$  and  $D_{7055}$ ). The addition of simultaneous photometry, absolute spectrophotometry, or spectra including temperature diagnostics in the range of  $T_Q$  could provide the third measurement needed.

For any  $f_S > 0$ ,  $T_Q$  must be greater than  $T_{\text{eff}}$ . Using our color versus  $T_{\text{eff}}$  calibrations, the mean  $(B-V)$  color implies  $T_Q \gtrsim 4700$  K. Its spectral type suggests a range of K2 V to K3 IV, or (interpolating from Gray 1988)  $5050 \text{ K} \gtrsim T_{\text{eff}} \gtrsim 4500$  K. Combining these estimates gives a conservative maximum range of roughly  $5100 \text{ K} \gtrsim T_Q \gtrsim 4500$  K. We then calculated  $f_S$  for all possible  $T_Q$  values spanning this range. We find that if  $T_S$  is

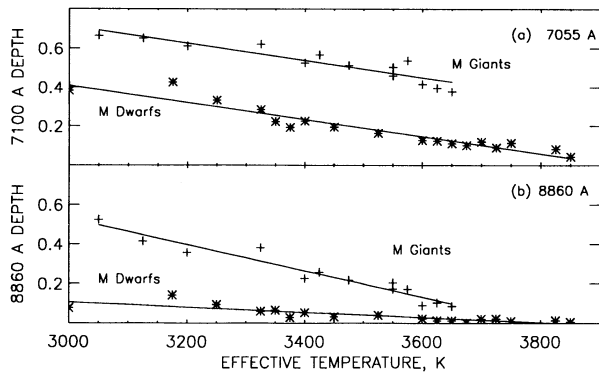


FIG. 5.—(a) Plot of 7055 Å band depth vs.  $T_{\text{eff}}$  M giant comparison stars (plus signs) and M dwarf comparison stars (asterisks). (b) Plot of 8860 Å band depth vs.  $T_{\text{eff}}$  for M giant comparison stars (plus signs) and M dwarf comparison stars (asterisks). Best-fit linear relationships are overplotted.

fixed, every 50 K increase in  $T_Q$  requires a  $\approx 1\%$  increase in  $f_S$  to match the observed band depths.

## 4. RESULTS

### 4.1. Spot Temperature

Our best-fit spot temperature for II Peg in 1989 October is  $T_S = 3500 \pm 200$  K. This quoted uncertainty reflects both the range of spot temperatures that provide reasonable fits to the II Peg spectra and the uncertainty in calculating the band depth ratio. Previous measurements of spot temperature on II Peg using photometry (Poe & Eaton 1985; Vogt 1981b; Byrne et al. 1987; Eaton 1992) have yielded values in the range  $3330 \text{ K} \leq T_S \leq 3700 \text{ K}$ . These methods have typically used quiet photosphere temperatures of  $4350 \text{ K} \leq T_Q < 4650 \text{ K}$ , at the lower end of our range. Estimates of spot “equivalent spectral types” of M6 III by Vogt (1981a) by M5 III by Huenemoerder & Ramsey (1987) suggest  $T_S \approx 3200 \text{ K}$ , though the range of effective temperatures spanned by stars classified as M5 III or M6 III makes this an approximate comparison.

### 4.2. Spot Filling Factor and Quiet Region Temperature

The spot filling factors,  $f_S$ , derived for II Peg (for a range of values of  $T_Q$ ) are given in Table 3. For 1989 October 12, the filling factor was derived solely from the 7055 Å depth, assuming a band depth ratio equal to the mean of those from other dates. If  $T_Q = 4800 \text{ K}$ , the filling factor varied from 54% at  $\Phi = 0.17$  to 64% at  $\Phi = 0.92$ . If  $T_Q = 4500 \text{ K}$ , the spot filling factor would range from 46% to 56%, and for  $T_Q = 5100 \text{ K}$  to filling factor would range from 61% to 72%. Figure 6 shows the filling factor as a function of orbital phase, calculated assuming  $T_S = 3500 \text{ K}$  and plotted for a range of quiet temperatures.

### 4.3. Comparison with Photometry

We can further refine our estimates of  $T_Q$  by taking advantage of contemporaneous photometry (Doyle et al. 1992a). II Peg was observed between 1989 July 20 and 1989 November 21, with two observations (HJD 2,447,807.382 and 2,447,811.388) falling in our observing interval. The latter appears to be affected by the flare. The first observation [ $V = 7.67$ ,  $(B-V) = 1.03$ ,  $(V-R)_{\text{KC}} = 0.61$ ,  $(R-I)_{\text{KC}} = 0.65$ ] was obtained at  $\Phi = 0.96$ , near photometric minimum on the rotational cycle immediately preceding our observations.

We constructed synthetic flux-calibrated spectra by combining the appropriate fractions (taken from the values of  $f_S$  given

in Table 3) of the relevant Kurucz models for each of the five phases at each of the three presumed values for  $T_Q$ . We then convolved these with the appropriate filter functions to predict  $(B-V)$ ,  $(V-R)$ , and  $(R-I)$  colors. Our results are shown in Figure 7. We find that the predicted values for  $T_Q = 4800 \text{ K}$  are consistent with the  $(B-V)$  and  $(V-R)$  colors, whereas  $T_Q = 4500 \text{ K}$  and  $T_Q = 5100 \text{ K}$  yield inconsistent colors. The TiO results for  $T_Q = 4800 \text{ K}$  predict  $(R-I)$  colors that are systematically slightly bluer than the observed photometry. Our interpretation is that the midrange  $T_Q$  is the correct value, but that we could be systematically underestimating  $f_S$  with our TiO technique. The most likely reason for this discrepancy is our use of M giant spectra as spot surrogates in the TiO analysis. The ideal spot proxies for II Peg, the (nonexistent) M subgiants, would have band depths intermediate between M dwarfs and giants, requiring larger  $f_S$  values to match the observations.

We attempted to derive independently the spot parameters using the synthetic photometry alone, taking a range of reasonable  $f_S$ ,  $T_Q$ , and  $T_S$  values. We found that all acceptable solutions to the various measured colors involve temperatures very close to those derived with the TiO analysis, but with a larger  $f_S$ . There likely are systematic errors in the synthetic photometry as a result of both the opacity known to be missing (particularly in the blue) from the cooler models and, to a lesser extent, our interpolations. The missing opacity will most strongly affect the  $(B-V)$  color, making it too “blue” for a given  $T_{\text{eff}}$ . We adopted an “optimal” photometric solution that most closely matches  $T_{V-R}$  and  $T_{R-I}$  but somewhat underestimates  $T_{B-V}$ . Our best solution has  $T_Q = 4850 \text{ K}$ ,  $T_S = 3500 \text{ K}$ , and  $f_S = 0.68\text{--}0.77$  (see Table 3).

The variation of  $f_S$  as a function of rotational phase is well determined regardless of  $T_Q$ . Doyle et al. (1992a) found a variation of approximately 0.45 mag in  $V$ , with a minimum at  $\Phi = 0.8$ . We find that a variation of  $f_S$  by 10% between the most and least spotted hemispheres could produce the observed spectra and their variations, and the star was always at least 50% covered with spots.

### 4.4. The 1989 October 11 Flare

On 1989 October 11 there was emission above the local continuum from the H I Paschen- $\theta$  (8862.8 Å) and Paschen- $\iota$

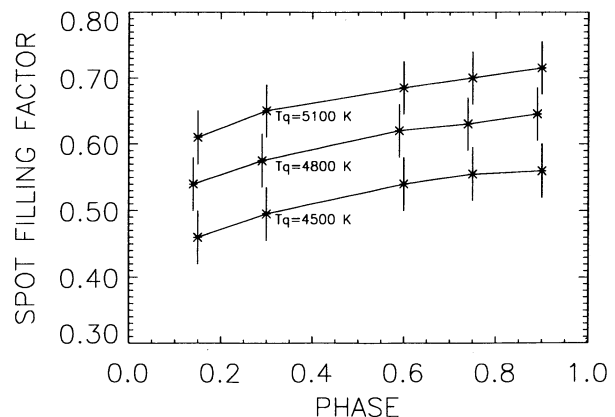


FIG. 6.—Spot filling factors,  $f_S$ , for II Peg as a function of phase, with  $T_S = 3500 \text{ K}$ . For clarity, the  $T_Q = 4800 \text{ K}$  curve has been slightly offset in phase. The three curves correspond to the different presumed values of  $T_Q$ . We consider  $T_Q = 4800 \text{ K}$  to be the most likely value.



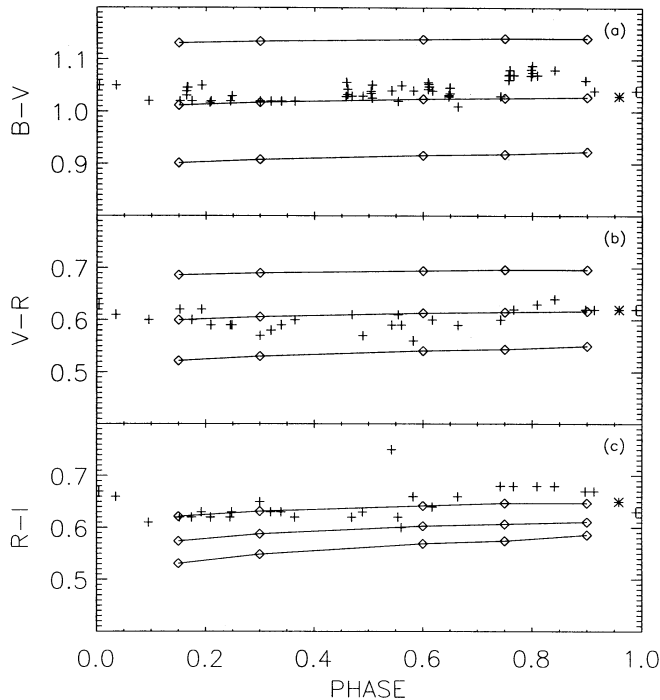


FIG. 7.—(a) A comparison between the observed ( $B-V$ ) colors from Doyle et al. (1992a; plus signs) and synthetic photometry predictions using the TiO results (i.e.,  $T_s = 3500$  K;  $f_s$  as given in Table 3). Top line is for  $T_Q = 4500$  K, middle line is for  $T_Q = 4800$  K, and lower line is for  $T_Q = 5100$  K. Only the  $T_Q = 4800$  K solution is consistent with the observed values. The asterisk represents the phase of an observation that was contemporaneous with our II Peg observations; the others were obtained over an interval of several months bracketing our observations. (b) Same as (a), but for ( $V-R$ ). (c) Same as (a), but for ( $R-I$ ). The  $T_Q = 4800$  K prediction is too blue, suggesting that  $f_s$  could be approximately 10% higher than determined by the TiO results alone.

(8750.5 Å) lines and from the He I (7065.2 Å) line. The emission equivalent widths, measured after subtracting the preflare spectrum from the flare spectrum, were  $0.74 \pm 0.05$  Å for H I Paschen- $\iota$ ,  $0.17 \pm 0.03$  Å for H I Paschen- $\theta$ , and  $0.24 \pm 0.03$  Å for He I  $\lambda 7065$ . There is also evidence for excess continuum emission caused by the flare. To our knowledge, this is the first flare observed so high in the H I Paschen series on an active star.

The ( $U-B$ ) color of II Peg on October 11 (HJD 2,447,811.388, about 0.5 day after our spectra) was still anomalously blue (0.52 compared to a more typical  $\sim 0.65$  at that phase; Doyle et al. 1992a). Whether the blue colors are caused by the same or by a second strong flare is impossible to determine.

## 5. DISCUSSION

Our spot filling factors,  $f_s$ , are weighted by projection and limb darkening. If the spot is near disk center, the true fractional area coverage (on the star),  $A$ , will be less than  $f_s$ , while for a spot near the limb,  $A > f_s$ . The amount of the over- or underestimate depends on the actual geometry and the value of  $A$  itself. In principle, a time series of  $f_s$  measurements can be used to constrain  $A$ , but additional assumptions about spot geometry would be needed to derive a unique solution.

The spot-to-quiet temperature ratio of II Peg ( $T_s/T_Q \approx 3500/4800 \approx 0.7$ ) is similar to the Sun ( $T_s/T_Q \approx 4000/5750 \approx 0.7$  in large umbrae; Allen 1976) and other active stars ( $0.65 \leq T_s/T_Q \leq 0.85$ ; Byrne 1992). The temperature difference is also

similar:  $\Delta T \equiv T_Q - T_s \approx 1300$  K for II Peg, while other active stars yield  $600 \text{ K} \leq \Delta T \leq 1800$  K, and the Sun shows  $\Delta T \approx 1800$  K for larger spots (Allen 1976).

Our derived spot parameters can be used to estimate what the unspotted surface of II Peg would look like. We find that  $T_Q$  implies a spectral type of about K1–2 IV for the unspotted surface, and  $V(f_s = 0) \approx 6.8$ . This is considerably brighter than the historical maximum,  $V = 7.2$  (Rucinski 1977), often assumed to be  $f_s = 0$  in photometric spot modeling analyses. Our results thus imply that II Peg is extremely spotted; dark umbra-like features actually cover more of the star than the “quiet” areas.

The literature is somewhat confusing concerning the sensitivity of TiO to luminosity. While some have claimed that TiO is “relatively” insensitive to luminosity (Wing & White 1978; Wing & Yorka 1979), narrow-band photometry does show a significant difference in the 7100 Å band between dwarf and giants, with giants generally showing more TiO absorption at a given  $T_{\text{eff}}$  and a steeper relationship between band strength and  $T_{\text{eff}}$  than dwarfs (Wing 1973, his Fig. 3; Wing, Dean, & MacConnell 1976, their Fig. 3). Our results generally support the latter view, although we find the slopes of  $D_{7050}^G$  and  $D_{7050}^D$  (but not  $D_{8860}$ ) versus  $T_{\text{eff}}$  to be quite similar.

We determined that M giants model the spotted regions of II Peg much better than M dwarfs, consistent with the evolved nature of the star. Comparison with synthetic photometry, however, suggests that giants overestimate the TiO absorption in the starspots on II Peg and thus underestimate  $f_s$ . Ideally, we would like to have a set of observations of inactive G and K subgiants to model the inactive regions of the photosphere of II Peg. M subgiants might also be very useful to test as spot models, but such stars do not exist.

In order to spectroscopically better determine  $T_Q$  and to determine  $T_s$  over a larger range, we must use more than the 200 Å spectrum bands included in this paper. We have begun a new phase of our observational program using the Penn State fiber-optic echelle spectrograph at Kitt Peak and the medium-resolution echelle spectrograph at Penn State’s Black Moshannon Observatory. These instruments allow us to observe the entire spectrum simultaneously with the same sensitivity as our existing observations. These spectra also will simultaneously provide a measure of the chromospheric activity level. We are currently developing a more sensitive spectral synthesis technique that would take these larger spectral regions into account in determining active star parameters.

There are still some difficulties in the analysis procedure that we must overcome before carrying out a full spectrum synthesis. One of the most difficult problems is normalizing the 7055 Å continuum for the coolest M-type comparison stars. There are other TiO bands and the atmospheric  $B$  band shortward of our  $\approx 200$  Å bandpass that could affect our normalization. There is weak evidence for spots on some of our comparison stars (Dorren & Guinan 1982), and surely most stars have some small fraction of spottedness. We must be wary of any anomalies in their spectra. Differing stellar metallicity could be a cause of scatter in our band depth calibration. Variable spectra in some of the late M giant stars could also cause scatter as a result of long timescale  $T_{\text{eff}}$  variations.

The original goal of this program was to derive a purely spectroscopic method to determine independently the area and temperature of starspots. To the extent that other stellar parameters are known, this has been a success.  $T_s$  was determined uniquely by the ratio of two TiO bands. Unfortunately,

the cataloged spectral types and colors, at least for II Peg, show such a range of uncertainty in  $T_Q$  that our measurement of  $f_S$ , from the absolute strengths of the bands, is not completely determined. For any reasonable  $T_Q$ , however,  $f_S$  was over 50% of the stellar surface, perhaps reaching 70%. In addition, the degree of variation of  $f_S$  with phase (10%) is independent of  $T_Q$ . Furthermore, spots are visible at all phases, and the previously determined "immaculate" level still includes at least  $\approx 35\%$  spot coverage.

## 6. CONCLUSIONS

We have developed a purely spectroscopic technique to determine the projected area coverage and temperature of photospheric spots on active stars, even if those spots are uniformly distributed on the stellar surface. We have applied this technique to spectra of II Peg obtained over six consecutive nights in 1989 October. With the help of contemporaneous

photometry, we find the best-fit values of  $T_Q = 4800$  K,  $T_S = 3500$  K, and  $f_S$  varying from 54% to 64% as the star rotates. Our result implies that II Peg, even at its historical maximum brightness ( $V \approx 7.2$ ), was covered by  $f_S \approx 34\%$ , making II Peg (and perhaps other active stars) much more spotted than previously realized.

This work was supported by NASA grants NAGW-2603 and NAG 5-2118 to The Pennsylvania State University and by NASA grants NAGW-112 and NAG 5-87 to the Harvard-Smithsonian Center for Astrophysics. D. B. O. was supported through a NASA Space Grant Fellowship at The Pennsylvania State University. We are especially grateful to the National Solar Observatory for providing a large amount of telescope time through the "solar-stellar" program, and especially Dave Jaksha and Paul Hartmann for their technical support. M. Mercadante assisted with the initial phase of data reduction. We are grateful to Larry Ramsey and David Huenemoerder for their continuing interest in our work.

## REFERENCES

- Allen, C. W. 1976, *Astrophysical Quantities* (London: Athlone)
- Andrews, A. D., et al. 1988, *A&A*, 204, 177
- Bessell, M. S. 1991, *AJ*, 101, 662
- Byrne, P. B. 1992, in *Surface Inhomogeneities on Late-Type Stars*, ed. P. Byrne & D. Mullan (Berlin: Springer), 3
- Byrne, P. B., Doyle, J. G., Brown, A., Linsky, J. L., & Rodonò, M. 1987, *A&A*, 180, 172
- Byrne, P. B., Panagi, P., Doyle, J. G., Englebrect, C. A., McMahan, R., Marang, F., & Wegner, G. 1989, *A&A*, 214, 227
- Campbell, B., & Cayrel, R. 1984, *ApJ*, 283, L17
- Cutispoto, G., & Rodonò, M. 1992, in *Surface Inhomogeneities on Late-Type Stars*, ed. P. Byrne & D. Mullan (Berlin: Springer), 267
- Dempsey, R. C., Linsky, J. L., Fleming, T. A., & Schmitt, J. H. M. M. 1993, *ApJS*, 86, 599
- Donati, J.-F., Brown, S. F., Semel, M., & Rees, D. E. 1992, in *Cool Stars, Stellar Systems, and the Sun*, ed. M. Giampapa & J. Bookbinder (ASP Conf. Series 26), 353
- Donati, J.-F., Semel, M., Rees, D. E., Taylor, K., & Robinson, R. D. 1990, *A&A*, 232, L1
- Dorren, J. D., & Guinan, E. F. 1982, *AJ*, 87, 1546
- Doyle, J. G., Butler, C. J., Byrne, P. B., Rodonò, M., Swank, J., & Fowles, W. 1989, *A&A*, 223, 219
- Doyle, J. G., Butler, C. J., Morrison, L. V., & Gibbs, P. 1988, *A&A*, 192, 275
- Doyle, J. G., et al. 1992a, *A&AS*, 96, 351
- Doyle, J. G., van den Oord, G. H. J., & Kellett, B. J. 1992b, *A&A*, 262, 533
- Drake, S., Simon, T., & Linsky, J. L. 1989, *ApJS*, 71, 905
- Eaton, J. A. 1992, in *Surface Inhomogeneities on Late-Type Stars*, ed. P. Byrne & D. Mullan (Berlin: Springer), 15
- Gliese, W. 1969, *Catalogue of Nearby Stars* (Karlsruhe: Verlag G. Braun)
- Gray, D. F. 1988, *Lectures on Spectral Line Analysis: F, G, and K Stars* (Arva, Ontario: The Publisher)
- Hartmann, L., Londoño, C., & Phillips, M. J. 1979, *ApJ*, 229, 183
- Hoffleit, D., & Jaschek, C. 1982, *The Bright Star Catalog* (4th ed.; Yale Univ. Obs.)
- Huenemoerder, D. P. 1988, in *Cool Stars, Stellar Systems, and the Sun*, ed. J. Linsky & R. Stencel (Dordrecht: Reidel), 512
- Huenemoerder, D. P., Buzasi, D. L., & Ramsey, L. W. 1990, in *Cool Stars, Stellar Systems, and the Sun*, ed. G. Wallerstein (ASP Conf. Series 9), 236
- Huenemoerder, D. P., & Ramsey, L. W. 1987, *ApJ*, 319, 392
- Huenemoerder, D. P., Ramsey, L. W., & Buzasi, D. L. 1989, *AJ*, 98, 2264
- Johnson, H. L. 1966, *ARA&A*, 4, 193
- Kurucz, R. L. 1991, in *Precision Photometry: Astrophysics of the Galaxy*, ed. P. Davis, A. Uggren, & K. Janes (Schenectady: L. Davis Press), 27
- Neff, J. E. 1991, *Mem. Soc. Astron. Italiana*, 62, 291
- Neff, J. E., O'Neal, D., & Saar, S. H. 1992, in *Inside the Stars*, ed. W. Weiss (ASP Conf. Series 40), 193
- O'Neal, D., Neff, J. E., & Saar, S. H. 1994, in *Cool Stars, Stellar Systems, and the Sun*, ed. J.-P. Caillault (ASP Conf. Series 64), 726
- Patterer, R. J., Vedder, P. W., Jelinsky, P., Brown, A., & Bowyer, S. 1993, *ApJ*, 414, L57
- Pettersen, B. R., & Hawley, S. L. 1989, *A&A*, 217, 187
- Poe, C. H., & Eaton, J. A. 1985, *ApJ*, 289, 644
- Ramsey, L. W. 1981, *AJ*, 86, 557
- Ramsey, L. W., & Nations, H. L. 1980, *ApJ*, 239, L121
- Ridgway, S. T., Joyce, R. R., White, N. M., & Wing, R. F. 1980, *ApJ*, 235, 126
- Rodonò, M., et al. 1986, *A&A*, 165, 135
- . 1987, *A&A*, 176, 267
- Rucinski, S. M. 1977, *PASP*, 89, 280
- Saar, S. H., Nordström, B., & Andersen, J. 1990, *A&A*, 235, 291
- Saar, S. H., & Neff, J. E. 1990, in *Cool Stars, Stellar Systems, and the Sun*, ed. G. Wallerstein (ASP Conf. Series 9), 171
- Saar, S. H., Piskunov, N. E., & Tuominen, I. 1992, in *Cool Stars, Stellar Systems, and the Sun*, ed. M. Giampapa & J. Bookbinder (ASP Conf. Series 26), 255
- . 1994, in *Cool Stars, Stellar Systems, and the Sun*, ed. J.-P. Caillault (ASP Conf. Series 64), 661
- Schwartz, D. A., Garcia, M., Ralph, E., Doxsey, R. E., Johnston, M. D., Lawrence, A., McHardy, I. M., & Pye, J. P. 1981, *MNRAS*, 196, 95
- Smith, M. A., & Giampapa, M. S. 1987, in *Cool Stars, Stellar Systems, and the Sun*, ed. J. Linsky & R. Stencel (Berlin: Springer), 477
- Smith, M. A., & Jaksha, D. 1984, in *Cool Stars, Stellar Systems, and the Sun*, ed. S. Baliunas & L. Hartmann (Berlin: Springer), 183
- Stauffer, J. R., & Hartmann, L. W. 1986, *ApJS*, 61, 531
- Strassmeier, K. G., Hall, D. S., Fekel, F. C., & Scheck, M. 1993, *A&AS*, 100, 173
- Tagliaferri, G., White, N. E., Doyle, J. G., Culhane, J. L., Hassall, B. J. M., & Swank, J. H. 1991, *A&A*, 251, 161
- Vogt, S. S. 1979, *PASP*, 91, 616
- . 1981a, *ApJ*, 247, 975
- . 1981b, *ApJ*, 250, 327
- Wing, R. F. 1967, in *Colloquium on Late-Type Stars*, ed. M. Hack (Trieste: Osservatorio Astronomico), 231
- . 1973, in *Spectral Classification and Multicolour Photometry*, ed. C. Fehrenbach & B. Westerlund (Dordrecht: Reidel), 209
- Wing, R. F., Dean, C. A., & MacConnell, D. J. 1976, *ApJ*, 205, 186
- Wing, R. F., & White, N. M. 1978, in *The HR Diagram*, ed. A. Phillip & D. Hayes (Dordrecht: Reidel), 451
- Wing, R. F., & Yorke, S. B. 1979, in *Spectral Classification of the Future*, ed. M. McCarthy, A. Phillip, & C. Coyne (Vatican City: Vatican Obs.), 519